Theoretical study of steam grown oxides as a function of temperature, pressure and p(O_2)

Hugh Davies and Alan Dinsdale

NPL Materials Centre, National Physical Laboratory
Teddington, Middlesex TW11 0LW, UK

Abstract

Depending on their history and composition stainless and 9/12 chrome steels can develop two types of protective oxide scale, comprising either a thin layer of chromium oxide or a more complex layer with the spinel structure. Both these types of scale are found in environments with low oxygen partial pressures such as in heat exchangers for power generation plant. This paper is concerned with the identification of the reason for these variations and to describe how the methods of equilibrium thermochemistry can be applied to systems so very far from equilibrium.

Background

The ability to model the behaviour of materials in different environments requires a generalised and reliable method for solving the chemical equilibrium problem involving many elements and phases. Some phases may be simple with fixed stoichiometry, however in general most phases will have variable composition (eg solid solutions). A general approach to this problem is to find the minimum in the Gibbs energy of the system by the redistribution of elements between possible phases. Expressed mathematically this becomes:

$$\underset{n}{Minimise} \quad G = \sum_{j=1}^{N} n_j \mu_j$$

such that $$\sum_{j=1}^{N} a_{ij} * n_j = r_i \qquad i = 1, 2 \ldots\ldots M \leq N$$

and $$n_j \geq 0$$

where

G is the Gibbs energy which is to be minimised by varying the values of the n_j, j = 1, 2,...N

n_j is the amount in moles of species j present in the system; each chemical substance with a different phase designation being considered as a distinct chemical species,

N is the number of species in the system,

μ_j is the chemical potential of species j, which may be a function of some or all of the species amounts in the same phase; it also depends on temperature and

pressure, (the form of μ_j depends on the model of the phase under consideration and is constructed such that $dG/dn_j = \mu_j$),

a_{ij} is the number of units of component i per species j,

M is the number of components in the system,

r_i is the number of moles of component i in the system.

The expression G is a non-linear function of the species amounts and is dependent on temperature, composition and pressure.

This optimisation problem can be solved using methods based on aspects of NPL's NOSL (Numerical Optimisation Software Library) library. It is a feature of this method that a lower value of the objective function (Gibbs energy) is found at the end of each iteration while maintaining feasibility with respect to the constraints - one reason that the method is so reliable. More details of the method may be found in Gill, Murray and Wright (1).

The methods described allow the calculation of phase and chemical equilibria in multiphase, multicomponent systems containing mixtures of gases, aqueous solutions, stoichiometric and solution phases (eg alloys, molten salts, oxides, polymers).

This has been implemented in software, MTDATA, developed at the National Physical Laboratory, which calculates equilibria using an extremely robust true Gibbs energy minimisation procedure developed by Hodson which requires no initial estimate of the equilibrium state (2). In this way MTDATA differs from many of the other chemical and phase equilibrium programs available. MTDATA has been recently described in some detail elsewhere (3).

A major barrier to the application of chemical equilibrium calculations to problems such as metal/oxide behaviour in steam environments is the availability and quality of the appropriate thermodynamic data. In this paper we present calculations using data from three main sources that address these issues in the area of complex gas species and oxide phase thermodynamic data.

The SGTE pure substance database (SGSUB) contains data for pure substances and gases. SGTE is a consortium of 13 leading centres involved in the development of high quality databases containing thermodynamic data for inorganic and metallurgical materials. For each substance, the data consist of:

- the enthalpy of formation at 298.15 K relative to the pure elements
- the standard entropy at 298.15 K and a pressure of 101325 Pa
- the temperature dependence of the heat capacity typically from 298.15 K
- temperatures and enthalpies of transition for non gaseous substances

These data allow the Gibbs energy of each substance to be calculated as a function of temperature and so enable MTDATA to perform phase equilibrium calculations and

tabulations. The present version of the pure substance database (version 10.0) contains assessed thermochemical data for over 4200 substances.

The NPL alloy database (MTSOL) which contains data for multicomponent, non-ideal phases for a wide range of metallic systems including steels. The database comprises expressions for the Gibbs energy (relative to the weighted sum of the enthalpies of the constituent elements) of the end-member species as a function of temperature and for the excess Gibbs energy for any solution phases formed between the end-member species. These expressions are derived from various thermodynamic models.

The NPL Oxide thermodynamic database (MTOX) is being developed via commercial sponsorship coordinated by the Mineral Industry Research Organization. Currently the database covers crystalline solutions, stoichiometric phases and liquid oxides in the K_2O-Na_2O-CaO-MgO-Fe-O-Al_2O_3-SiO_2 system with additions of ZnO, Cu-O, B_2O_3, MnO, ZrO_2, PbO, Cr-O, NiO, Li_2O, Cu-Fe-Ni-S-O mattes and metallic phases, and dilute solutions of S, SO_4^{2-}, OH^-, F-, PO_4^{3-} in selected liquid oxides.

The current round of this project started in December 2002. New oxides to be added include Nb_2O_5, V_2O_5 and P_2O_5. Solutions involving CaF_2 are also being modelled. In an associated DTI project Co additions to matte/metal phases and CoO additions to oxide phases are being considered. The feasibility of modelling volume changes in oxide phases, the viscosity of oxide liquids and critical cooling rates for glass formation is also being investigated.

Data assessment

During the process of critical assessment all the experimental phase diagram and thermodynamic data for a given system are analysed carefully and a set of parameters derived to represent the thermodynamic properties of all phases which are consistent with the totality of the experimental information. This involves a process of optimisation during which the differences between the calculated and observed properties are minimised by tuning the parameters. It should be emphasised that this is not a simple curve fitting process since measurements of a wide range of different properties must be consistent as a result of underlying thermodynamic relationships.

The optimised parameters pertain to specific models to represent the variation of Gibbs energy of phases with temperature, pressure and composition. For most calculations it is usual to assume that the gas phase consists of an ideal mixture of chemical species – the data then relate to variation of enthalpy, entropy and heat capacity with temperature. Under extreme conditions eg at very high pressures the gas may be anything but ideal and in that case a more sophisticated approach is required. For most pure substances, either gaseous, liquid or crystalline, the general form of expression for the variation of Gibbs energy with temperature is:

$$^{o}G_T = a + bT + cT\ln T + \sum dT^n$$

where the enthalpy, entropy and heat capacity contributions can be obtained by differentiation.

The thermodynamic properties of the fcc and bcc alloy solid solution phases eg for the Cr-Fe system, are modelled according to the expression:

$$G = x_{Cr}G_{Cr} + x_{Fe}G_{Fe} + RT(x_{Cr}\ln x_{Cr} + x_{Fe}\ln x_{Fe}) + G^{xs} + G^{mag}$$

where G^{xs}, the excess Gibbs energy, is represented using the Redlich-Kister equation :

$$G^{xs} = x_{Cr}x_{Fe}(L_0 + L_1(x_{Cr} - x_{Fe}) + L_2(x_{Cr} - x_{Fe})^2 .....)$$

and G^{mag}, the magnetic contribution given by:

$$G^{mag} = RT\ln(\beta + 1)\ g(\tau)$$

where β is the average magnetic moment per atom, τ given by

$$\tau = T / T^*$$

where T* is the critical temperature (the Curie temperature for ferromagnetic materials or the Nèel temperature for antiferromagnetic materials) and g(τ) given by:

$$g(\tau) = 1 - \left[\frac{79\tau^{-1}}{140p} + \frac{474}{497}\left(\frac{1}{p} - 1\right)\left(\frac{\tau^3}{6} + \frac{\tau^9}{135} + \frac{\tau^{15}}{600}\right)\right] / D \qquad \tau \le 1$$

$$g(\tau) = -\left[\frac{\tau^{-5}}{10} + \frac{\tau^{-15}}{315} + \frac{\tau^{-25}}{1500}\right] / D \qquad \tau > 1$$

where $D = \frac{518}{1125} + \frac{11692}{15975}\left(\frac{1}{p} - 1\right)$

The value of p is the fraction of magnetic enthalpy absorbed above the critical temperature and depends of the structure. For bcc phases p = 0.4 while for other common phases p = 0.28.

The average magnetic moment, β, and the critical temperature, T^*, vary with composition:

$$\beta = x_{Cr}\beta_{Cr} + x_{Fe}\beta_{Fe} + x_{Cr}x_{Fe}(\beta_0 + \beta_1(x_{Cr} - x_{Fe}) + \beta_2(x_{Cr} - x_{Fe})^2 .....)$$

$$T^* = x_{Cr}T^*_{Cr} + x_{Fe}T^*_{Fe} + x_{Cr}x_{Fe}(T^*_0 + T^*_1(x_{Cr} - x_{Fe}) + T^*_2(x_{Cr} - x_{Fe})^2 .....)$$

For oxide systems it is necessary to use models with rather greater complexity to represent the ionic nature of the material and the lattice structure of the crystalline phases. Typically this means use of models such as the ionic liquid, associated solution or quasichemical models for the liquid phase where the thermodynamic properties may vary sharply over small ranges in composition reflecting short range ordering effects. For the crystalline phases the compound energy model is normally used which allows the introduction of non-stoichiometry, lattice vacancies, interstitial ions and exchange of ions between different sublattices in a formally very simple way. So, for example, for the assessment of data for the Cr-Fe-Ni-O system, Taylor and Dinsdale (4) represented the halite phase which incorporates the compositions pertaining to wustite and bunsenite (NiO) by:

$$(Cr^{3+}, Fe^{3+}, Fe^{2+}, Ni^{3+}, Ni^{2+}, Va)\ (O^{2-})$$

where the two sublattices have equal numbers of sites. Vacancies (Va) were introduced into the cation sublattice to allow the phase to become oxygen rich. In this case the properties of the phase are represented in terms of unaries or "compounds" formed by taking all combination of ions from the different sublattices. The overall Gibbs energy is then calculated in terms of the site fraction of the cations in the first sublattice and the Gibbs energies of these "compounds", with additional terms to take account of the ideal and non-ideal mixing of the cations.

The spinel phase is rather more complicated to model. Firstly it is necessary to consider 4 distinct sublattices, tetrahedral and octahedral sublattices for the cations, an interstitial sublattice to account for deviations from stoichiometry and a sublattice for the oxygen anions. For the Cr-Fe-Ni-O spinel which covers the composition ranges of magnetite, Cr_3O_4, nickel chromate, iron chromate and nickel ferrite and this can be thought of in terms of:

$$(Cr^{3+}, Cr^{2+}, Fe^{3+}, Fe^{2+}, Ni^{2+})\ (Cr^{3+}, Fe^{3+}, Fe^{2+}, Ni^{2+}, Va)_2\ (Fe^{2+}, Va)_2\ (O^{2-})_4$$

where the first two sets of brackets represent tetrahedral and octahedral sites and the third set of brackets represents an interstitial sublattice. There is a large number of unary or "compound" combinations formed by taking cations in turn from each of the sublattices, many of which are electrically charged. Various rules and exchange energies were employed to define values for the Gibbs energies of these "compounds".

The approach allows the calculation of distribution of cations between the octahedral and tetrahedral sites and this can be compared against any experimental information where available. Figure 1 shows how this is predicted to vary between Fe_3O_4 and $FeCr_2O_4$ at 1000 K.

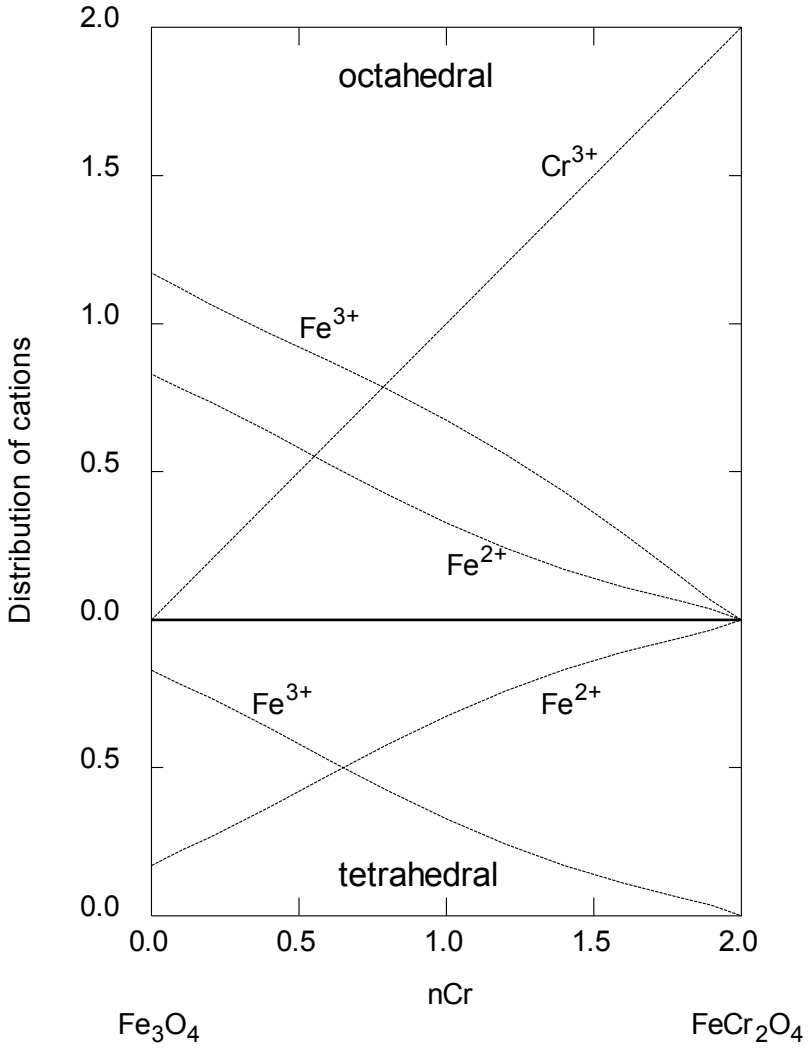

Figure 1. Calculated distribution of Fe and Cr ions between octahedral and tetrahedral sites at 1000 K as the spinel composition changes from Fe_3O_4 to $FeCr_2O_4$. The lower part of the diagram shows the distribution of cations in the tetrahedral sites which, for this composition range, is occupied completely by ferrous and ferric ions. The upper part of the diagram shows the site distribution on the octahedral sublattice.

The corundum phase which covers the composition range between haemetite Fe_2O_3 and Cr_2O_3 was modelled in a similar way in terms of:

$$(Cr^{3+}, Cr^{2+}, Fe^{3+})_2 \, (Cr^{3+}, Ni^{2+}, Va) \, (O^{2-})_3$$

Once the overall set of data have been derived for a given system it is possible to undertake a range of calculations to model a variety of phenomena. For example Figure 2 is a calculated phase diagram for 1473 K in which the ordinate shows the oxygen potential expressed as the $\log_{10}p(O_2)$ and the abscissa shows the mol fraction of Cr in the total Cr + Fe irrespective of the proportion of oxygen. The structure of the diagram is exactly equivalent to a temperature - composition binary diagram. On this diagram the experimental data of Snethlage and Klemm (5) are superimposed.

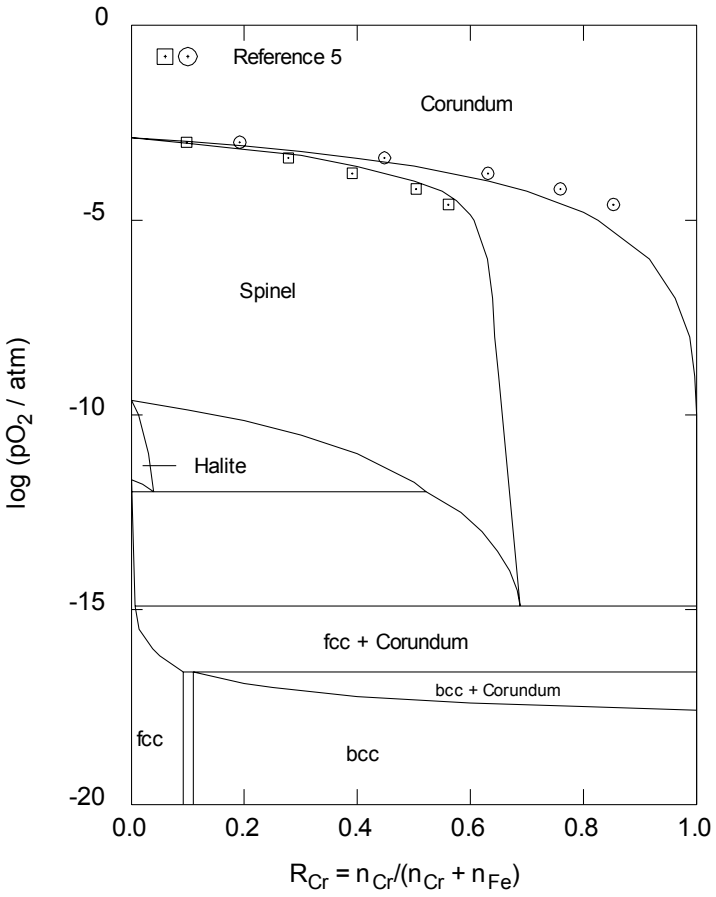

Figure 2 Calculated pO_2 – composition diagram for the Cr-Fe-O system at 1473 K

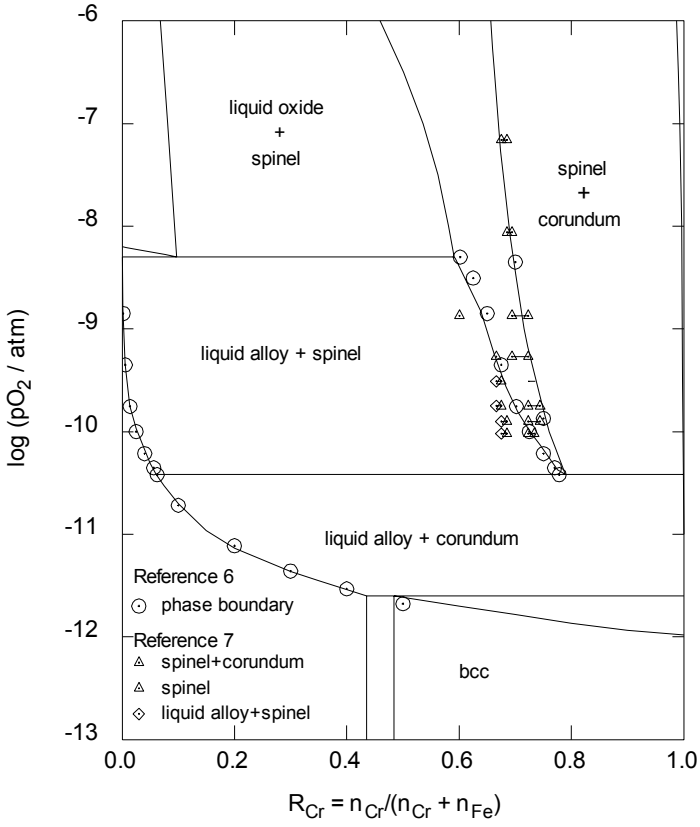

Figure 3. Calculated pO_2 – composition diagram showing experimental phase compositions at 1873 K.

Figure 3 shows the equivalent diagram for 1873 K. While these temperature are very much higher than of use for modelling the corrosion of heat exchanger tubes the diagrams do demonstrate that the critically assessed data have been derived from experimental properties measured over a wide range of conditions often quite remote from any single application. Diagrams similar to Figures 2 and 3 can be of much use in understanding and interpreting corrosion phenomena as will be shown later in this paper.

Calculation of gas phase speciation and metal volatility in steam

Later in this paper use will be made of the partial pressure of oxygen (as $O_2(g)$) as a measure of the oxidation state of the system. With knowledge of the oxygen partial pressure it is then possible, for various alloy compositions, to predict which oxide phases may potentially form as corrosion products.

In a pure steam environment oxygen may be formed by the thermal decomposition of water molecules. Figures 4a and 4b show the calculated oxygen partial pressures in equilibrium with steam, modelled as an ideal gas at a number of different total pressures, as a function of temperature and pressure and also (in Figure 4b) the equilibrium pressures at which iron oxides (Fe_2O_3, Fe_3O_4 and FeO) become stable. All data were taken from the SGTE Substance Database v10.0.

It is clear that the oxygen partial pressure produced by steam at all temperatures and pressures shown is capable of stabilising an oxide coating on iron. The formation of complex oxide coatings containing iron, chromium and nickel will be discussed in greater detail later in this paper.

In a high-pressure steam environment it is also possible that gaseous species containing metallic elements such as iron and chromium could be produced with sufficiently high partial pressure to provide a mechanism for alloy degradation.

At a pressure of 1 atm (Figure 5a) the highest predicted partial pressure (species $Fe(OH)_2(g)$) is likely to be too low to cause significant loss of iron to the gas phase. However Figure 5b shows, that at 340 atm, the partial pressure of $Fe(OH)_2(g)$ is predicted to approach value of 10^{-5} atm. The behaviour of chromium volatilisation, shown in Figures 6 (a) and (b) is generally similar to that predicted for iron, however at all steam pressures and temperatures the partial pressures of chromium containing gaseous species are predicted to be very low and therefore volatilisation is unlikely the be a significant degradation mechanism.

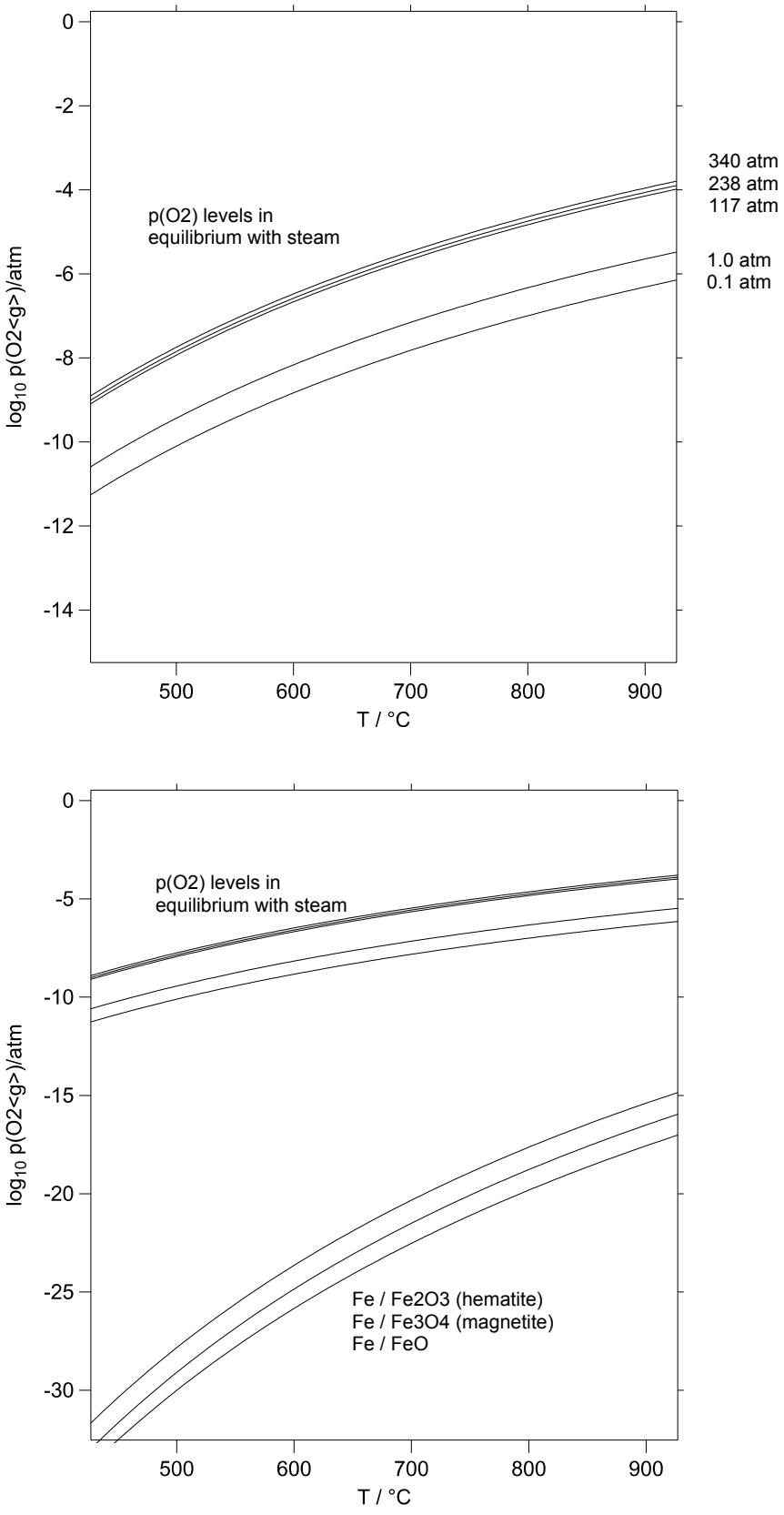

Figure 4 (a) Calculated oxygen partial pressure in equilibrium with steam at various pressures (b) Calculated oxygen partial pressures required to form various iron oxides.

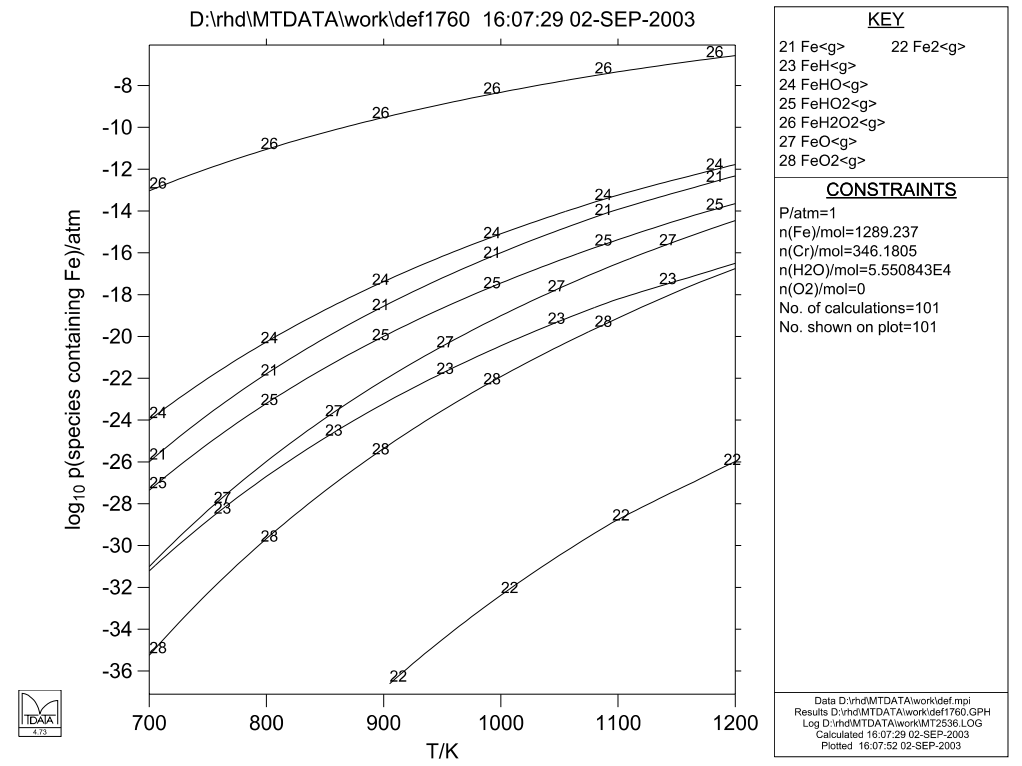

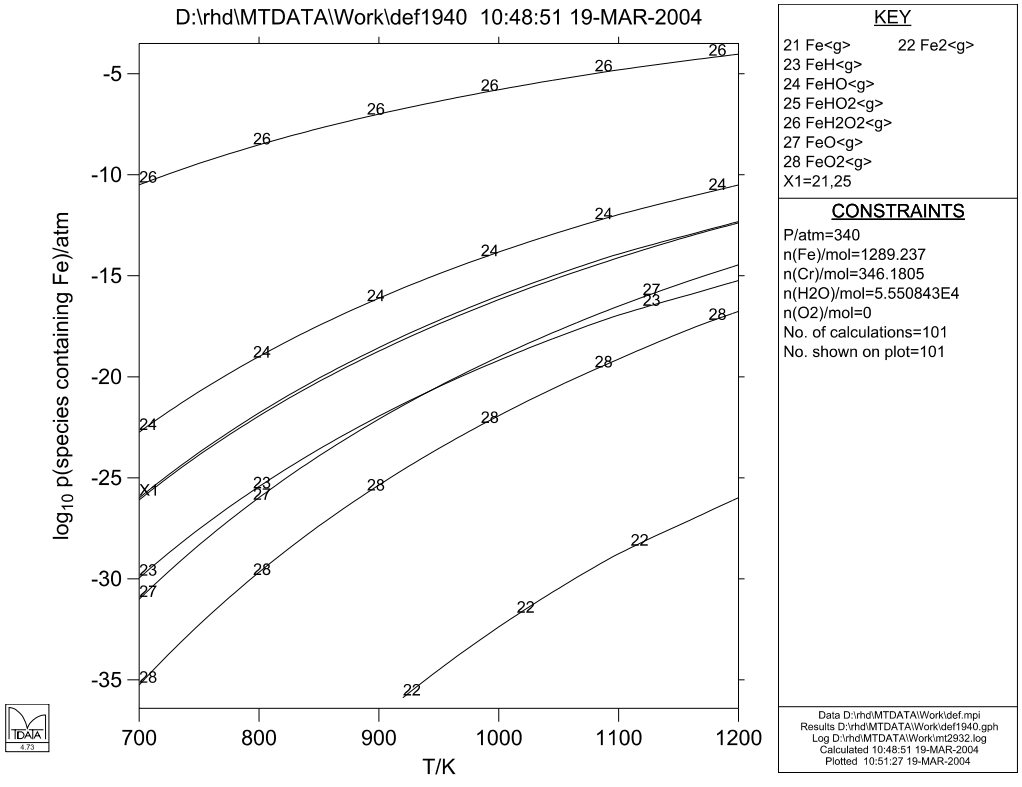

Figures 5 Calculated partial pressures of gaseous iron containing species in a steam environment at a pressure of (a) 1 atm and (b). 340 atm respectively

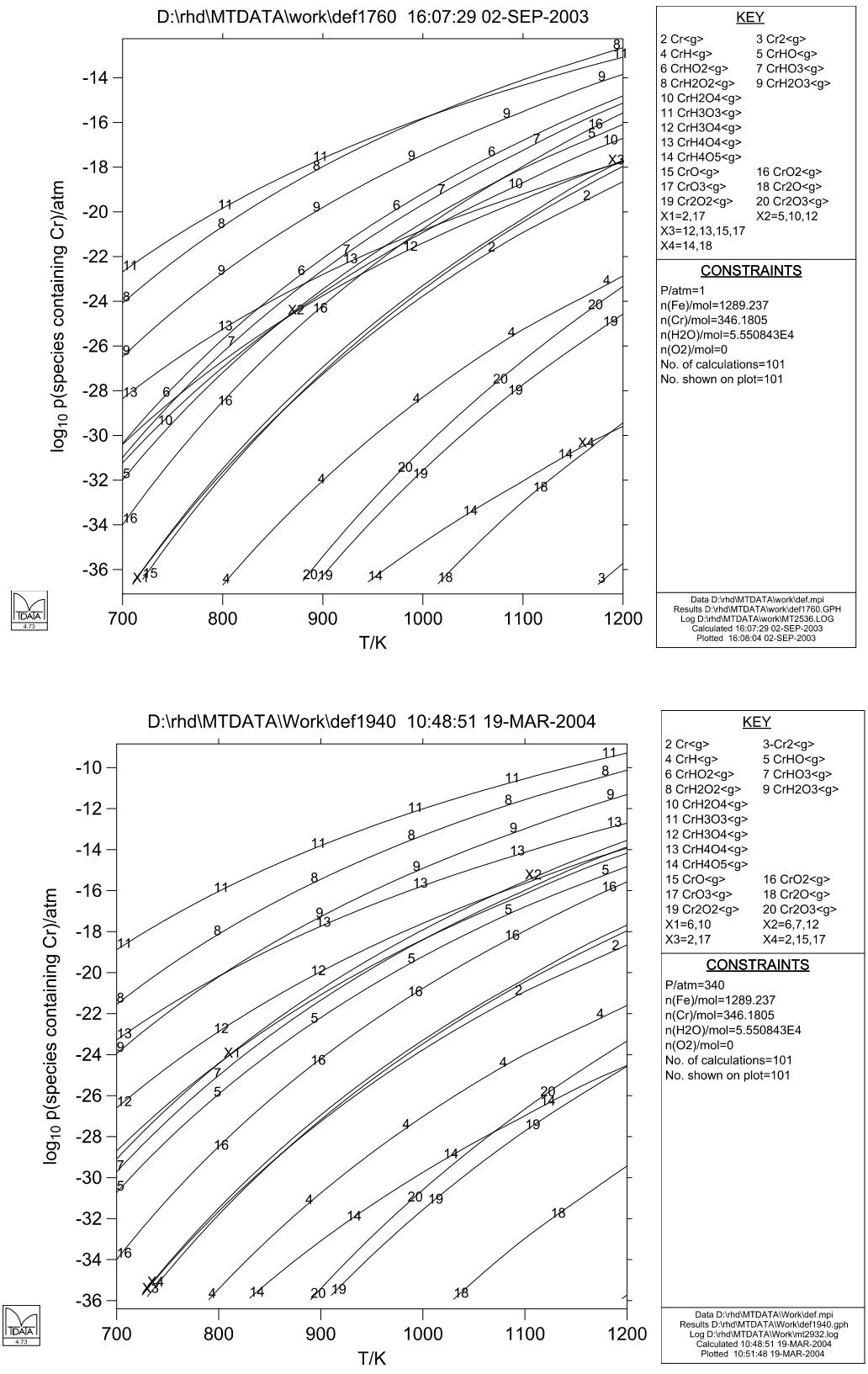

Figures 6 Calculated partial pressures of gaseous chromium containing species in a steam environment at a pressure of (a) 1atm and (b) 340 atm respectively

Analysis of the formation of the oxide scale

A useful introduction to high temperature corrosion has been given by Kofstad (8) and a description of the oxide scales found on 316-type steels by Rowlands and Manning (9). The thermodynamic analysis of corrosion of iron-chromium-nickel alloys has been considered by Barry and Chart (10) and Rahmel et al (11) and considerably extended by Barry and Dinsdale (12). Before considering why the deposition is selective it is necessary to examine the origin of the two different types of oxide scale. However, a complete analysis of the scale formation is not possible at present for many reasons.

- The Fe-Cr-Ni-O system has three metallic components, the proportions of which are not constant through the surface region of the alloy and the overlying oxide. This makes the representation of the results very difficult in two dimensions.
- Thermodynamic equilibrium may not be achieved even at a local level.
- Flaws may be present in the alloy from the outset or may be induced by the corrosion itself (13).
- Electrical double layers may be present within the semiconducting oxide phases in contact with each other or the metal.
- The outward diffusion of the alloy components and/or the inward diffusion of oxygen are unlikely to take place homogeneously through the grains of the oxide. Diffusion probably occurs preferentially along grain boundaries and other extended defects.
- The contribution of surface energies may also be important in phase stabilisation.

For these reasons it is necessary to simplify the problem.

- The normal principle will be followed that, except where otherwise stated, equilibrium is maintained wherever phases come in contact, whereas within phases there may be gradients in composition and thermodynamic potential.
- The effects of surfaces will be ignored on the basis that the solubility of a component in a grain boundary is likely to be related to its solubility in the adjacent phase.
- The most important simplification is initially to reduce the number of components, by omitting the nickel and beginning with oxidation of binary Fe-Cr alloys.

Formation of corundum scales in the Fe-Cr-O system

Chromium imparts corrosion resistance to steels by the formation of a passivating oxide at very low oxygen potentials. At 900 K the Cr^{3+} ions diffuse only very slowly through interstitial positions in the oxide lattices and grain boundaries (14). A more general description of the modelling and applications of data on oxides is given by (15).

As indicated by Figures 7 and 8, an iron-chromium alloy containing less than 23 mol% Cr will be single phase ferrite (bcc) at 900 K.

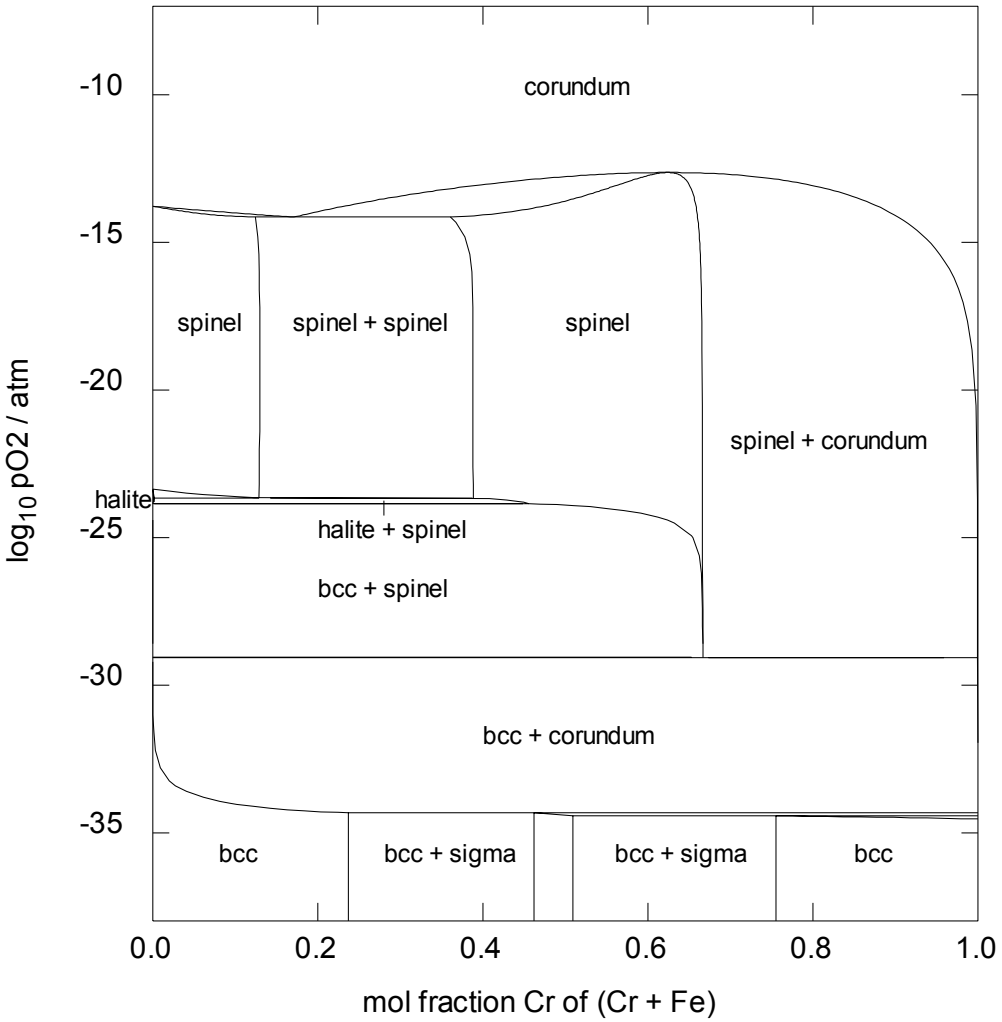

Figure 7 Calculated phase equilibria at 900 K in the Fe-Cr-O system as a function of oxygen potential and mol fraction of Cr in (Fe + Cr). 900 K is close to the lower temperature limit of wüstite (named here for generality halite), which therefore has a barely visible phase field on this scale. The other phases are corundum, a solution of Cr_2O_3 and Fe_2O_3; spinel and the metallic sigma phase.

Triangular three-phase regions on Figure 8 correspond with invariances (horizontal lines) on Figure 7. The corners of the triangles provide a useful point of reference, because they correspond with nodal points on the invariant lines of Figure 7. The diagrams predict that when the alloy is exposed to oxygen an oxide layer will form with the corundum structure and a composition very close to Cr_2O_3. If the composition of the alloy adjacent to the oxide were to remain unchanged, the oxygen potential there would be $10^{-34.5}$. Although Fe_2O_3 is isostructural with Cr_2O_3, because iron oxidises only at much higher oxygen potentials, the extent of its solution in the corundum phase will be very low. For the same and also for structural reasons, the solubility of FeO will also be low. Diffusion of iron through the Cr_2O_3 is therefore very slow for two reasons, the diffusion rates of cations in Cr_2O_3 are inherently low and in any case almost no iron

ions are present in solution at low oxygen potentials. For these reasons the oxide layer tends to be very thin and close to Cr_2O_3 in composition throughout its thickness.

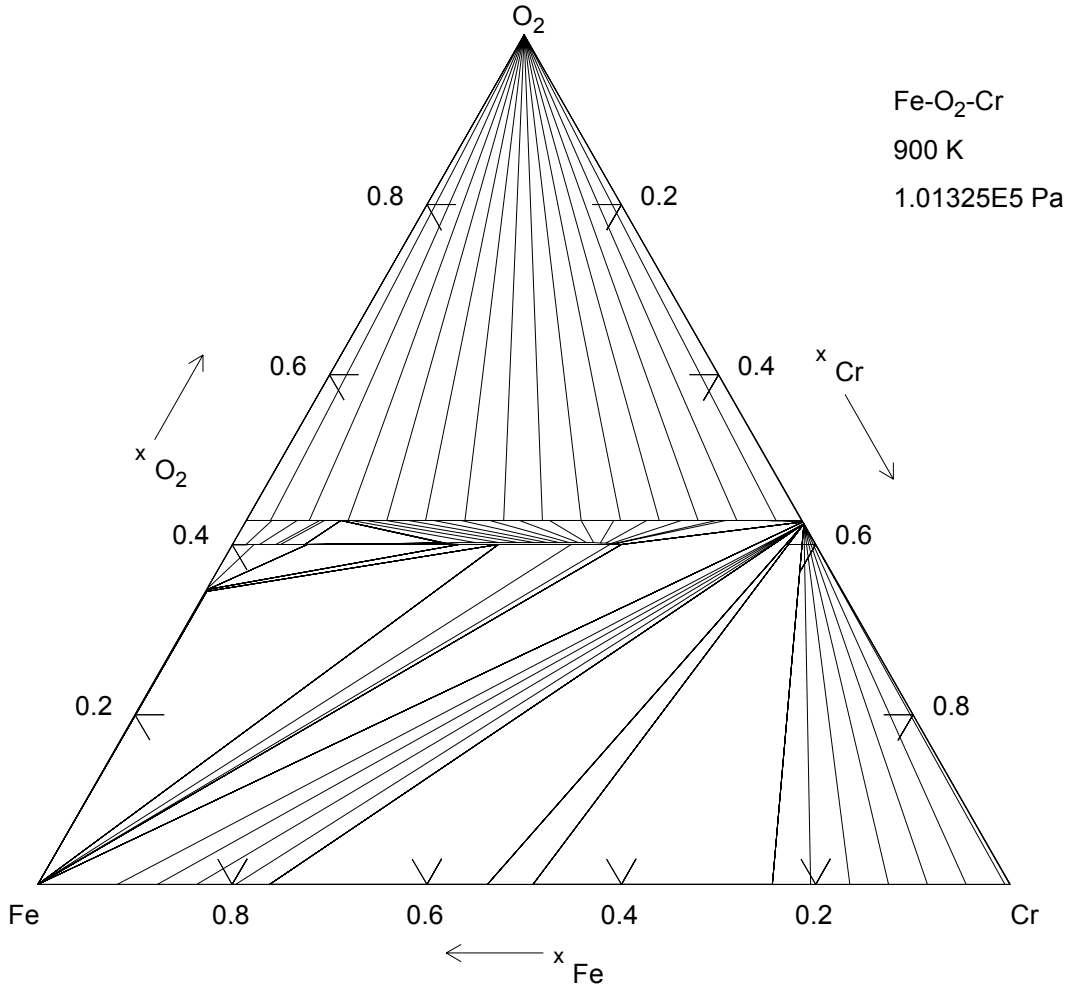

Figure 8 Calculated phase diagram at 900 K for the Fe-Cr-O system. The triangles are three-phase regions within which the three coexisting phases have individually constant compositions and the activities of the components, including oxygen, are constant. The phases on the Fe-O binary are halite (wüstite), spinel (magnetite) and corundum (haematite), solution in which extends to Cr_2O_3.

The same arguments can be applied to the formation of corundum scales on alloys containing nickel as well as iron and chromium. The "stainless", often mirror-like appearance of alloys such as the 316 series (circa 10 wt% Ni, 18 wt% Cr) depends on the very thin character of the oxide film. These steels are austenitic rather than ferritic because, as shown by Figures 9 and 10, the stable alloy phase at 900 K is fcc rather than bcc. The Ni-Cr-O system is of less significance for oxidation of steels because, for reasons discussed below, the nickel and chromium concentrate in different phases.

Formation of spinel scales

Depletion of chromium in the surface of steels during oxidation of steels is likely to be marked because the diffusion rate of chromium is known to be slow. Calculations for

the Fe-Cr-O system show that if the depletion of chromium is sufficient to cause the concentration to fall to about 0.01% (not visible on the scale of Figure 7), a spinel approximating in composition to $FeCr_2O_4$ would be the stable oxide product rather than corundum. In practice the chromium concentration in the depleted alloy at which spinel will form rather than corundum is likely to be very considerably greater than this, because spinel is much more tolerant of solid solution, for example of manganese which is a minor component of the steel. Moreover, because the driving force for the oxidation of bare metal is so large, a great variety of processes may occur, the only thermodynamic limitation being that the Gibbs energy should be lowered. There is good evidence that the formation of spinel is favoured over corundum under such conditions. For example, when alumina is quenched from high temperature gas streams, γ-alumina, which has a disordered spinel structure, is formed rather than α-alumina, which has the corundum structure (16).

For stainless steels the Cr_2O_3 layer that forms is sufficiently coherent for it to act as an effective corrosion resistant passivating layer. For 9/12 chrome steels, however, the level of chromium is insufficient to form a layer which is sufficiently coherent to provide the necessary oxidation resistance. In such circumstances iron atoms can still be exposed to the oxidising atmosphere and these can react with any Cr_2O_3 present to form the spinel phase with the approximate composition of $FeCr_2O_4$. Any further iron could oxidise to form first wüstite (halite) and then a magnetite rich spinel on top of the $FeCr_2O_4$ rich spinel.

Another factor that will tend eventually to result in the formation of spinel scales is repeated cracking of corundum scales. So long as the layers remain impervious the composition of the alloy adjacent to the oxide will gradually be restored by diffusion in the alloy. However, repeated breakdown and renewal of the scale further depletes the chromium and will eventually lead to formation of spinel type scales.

Figures 7 and 8 show that at 900 K the iron-chrome spinel and magnetite are only partially miscible. In principle the two spinels, one chromium-rich and one iron-rich, can coexist over a range of oxygen potential but in practice this probably does not happen. Figure 7 shows that only the iron-chrome spinel is stable at the lowest oxygen potentials closest to the alloy surface. In nickel free steels this is overlaid by a spinel close in composition to magnetite, Fe_3O_4.

In comparison with iron, nickel will be concentrated in the alloy because this is favoured by the reaction:

$$Fe + NiCr_2O_4 = Ni + FeCr_2O_4$$

The effect of this is to inhibit diffusion of nickel through the spinel to outer layers where the oxygen potential is higher. Moreover, as discussed by Cox et al. in relation to diffusion and partition of elements in oxide scales on alloys (17), the Ni^{2+} ion, which has eight 3d electrons, has (like Cr^{3+}, which has three) a strong preference for the octahedral sites in the spinel structure and diffuses with difficulty through intervening

tetrahedral sites. In agreement with this line of argument, the outer layers, which are in contact with the gaseous atmosphere and therefore see an oxygen potential of about 1.77×10^{-20} ($10^{-19.75}$), are known to have a composition close to magnetite. This is because the chromium is confined to regions of the oxide scale near the alloy surface by the low rates of diffusion of the Cr^{3+} ions and the nickel remains in the alloy for the reasons given above.

Figure 7 may give the misleading impression that the alloy coexists in the scale with a variety of oxides over a range of oxygen potentials. If the oxide film is coherent this is clearly not the case. The oxide film adjacent to the alloy, whether corundum or a chrome-rich spinel, effectively cuts off the alloy from exposure to oxygen potentials higher than that defined by coexistence of the alloy and the particular oxide scale. However, the occurrence of cracking does allow further contact between the alloy and the atmosphere as discussed below.

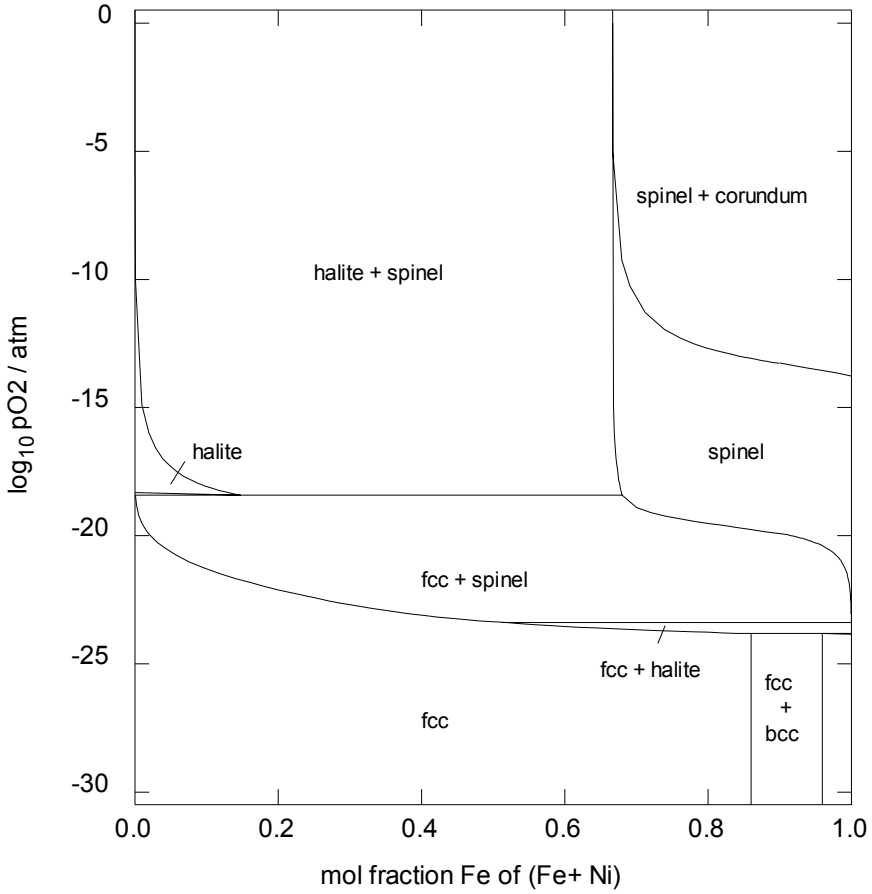

Figure 9 Calculated phase equilibria at 900 K in the Ni-Fe-O system as a function of oxygen potential and mol fraction of Fe in (Ni + Fe). The halite phase of nickel oxide dissolves a up to about 15 mol % of iron oxide but is nevertheless unstable at the oxygen potential of the gas atmosphere $10^{-19.75}$. However, the spinel phase can take up a substantial proportion of nickel.

The effect of cracks in the scales on the behaviour of nickel

Cracking and potentially spalling of the oxide scale will expose the metal, now depleted of chromium and, in the presence of spinel scales, somewhat enriched in nickel, to higher oxygen potentials. For both types of scale cracks can act as pipes through which nickel can diffuse to the outer layers of the scale. The difference for the two types of scale is that the spinel scale has an outer layer of magnetite with which any nickel formed can readily react with to form a solid solution, whereas the corundum (Cr_2O_3) scale will, for reasons connected with the low mobility of Cr^{3+} ions, be unreactive to nickel. Furthermore the formation of nickel oxide as a new phase is thermodynamically impossible, because the oxygen potential is marginally too low.

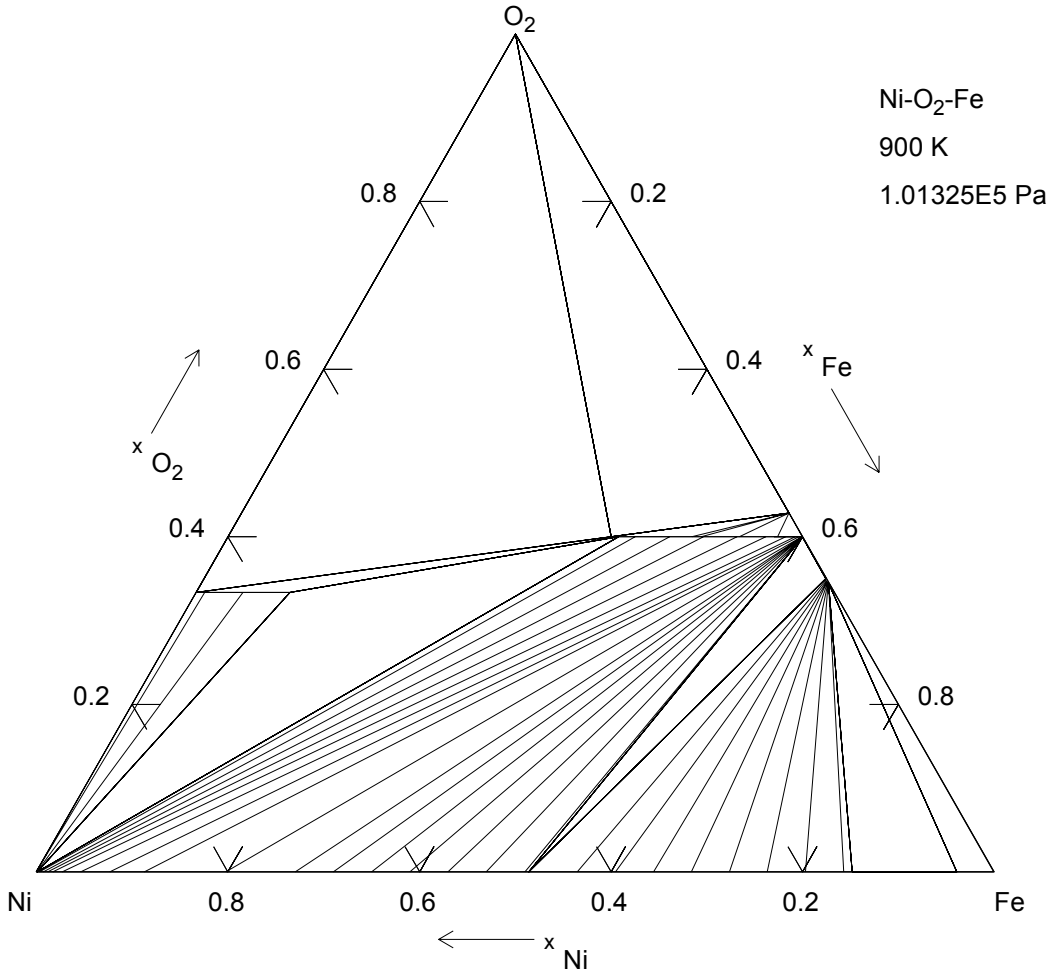

Figure 10 Calculated phase diagram for the Fe-Ni-O system at 900 K. This diagram and Figure 9 have the same relationship as Figures 7 and 8.

The two reactions concerned are:

$2\ Ni + O_2(g) = 2\ NiO$ $(\log_{10}K_{900} = 18.31)$ 1

$3/2\ Ni + O_2(g) + Fe_3O_4 = 3/2\ NiFe_2O_4$ $(\log_{10}K_{900} = 18.90)$ 2

Because $\log_{10}p(O_2)$ at the outer oxide surface is -19.75 reaction 1 cannot occur, since a

higher value of -18.31 would be needed for pure NiO to be stable. Moreover, the solution of iron oxide into NiO would not significantly modify this value, because the lower boundary to the Ni-rich halite region of Figure 9 is very flat. On the other hand the reaction 2 can occur provided the proportion of nickel in the spinel phase remains even moderately low.

The maximum proportion of nickel that can be absorbed by the spinel at this oxygen partial pressure corresponds with $(Ni_{0.13}Fe_{0.87})_3O_4$, as can be read off from Figure 9 at $\log_{10}p(O_2) = 19.75$. Only if the amount of nickel at the surface were greater than this would a nickel-rich fcc alloy coexist with the spinel. It is not necessary to take into account the presence of the chromium in computing the equilibria on the spinel scales because, for reasons already stated the outer spinel layer is essentially chromium free. These arguments provide a reason why free nickel does not persist on the spinel scales, whereas once present on the corundum type scales, it tends to persist. The remaining point of greatest doubt concerns the mechanism whereby nickel-rich material gets to the surface. This could possibly arise if any sulphur present is able to transport nickel to the surface.

Conclusions

Corrosion and deposition are topics on which there is an enormous amount of experimental information and scientific knowledge. The complexity of the processes is great because there are many possible processes that may operate in series or in parallel. Moreover, as if the analysis was not complex enough for a ternary alloy, 316 type stainless steels usually contain significant proportions of manganese and silicon which are known to influence corrosion behaviour. For all these reasons at the present time thermodynamic methods cannot be used ab initio to solve problems in corrosion. Rather they should be used to provide a basis on which to test ideas indicated by experiment and human imagination and thereby as a means for designing more definitive experiments.

The effect of increased steam pressure on corrosion rates is likely to be the result of one or more kinetic factors as thermodynamically the oxygen partial pressure predicted in even 1 atm steam is sufficient (fig 4b) to form Fe_2O_3 or more complex oxide phases. In high pressure steam volatility of $Fe(OH)_2(g)$ (fig 5b) may also indicate a mechanism, however below 1000 K the effect is probably small.

A more challenging approach would be to combine the thermodynamic calculations outlined here with a finite difference model to account in a quantitative manner for the growth of oxide scales on the surface of the steel and diffusion of the metallic ions and oxygen ions through the bulk and along the grain boundaries.

References

1 Gill P, Murray W, Wright M, Practical Optimisation, Academic Press, London 1981.

2 A T Dinsdale, S M Hodson, T I Barry, J R Taylor, Computer Software in Chemical and Extractive Metallurgy, (Pergamon Press, Oxford, 1989), pp59-74

3 Davies R H, Dinsdale A T, Gisby J A, Robinson J A J, Martin S M, CALPHAD, 26(2), 2002, pp. 229-271

4 Taylor J R, Dinsdale A T, Z. Metallkunde, 1993, 84, 335-345.

5 Snethlage R, Klemm D D; Neues Jahrb. Mineral. Abh. 1975, 125, 227-242

6 Toker N Y; "Equilibrium Phase Relations and Thermodynamics for the systems Chromium-Oxygen and Iron-Chromium-Oxygen in the temperature range 1500-1825°C" Ph.D Thesis, Pennsylvania State Univ., 1978.

7 Iwamoto N; Takano M; Adachi A; Tech. Rept. Osaka Univ. 1968, 18, 37-44

8 Kofstad P, "High Temperature Corrosion", 1988, Elsevier Applied Science, London.

9 Rowlands R C, Manning M I, in "High Temperature Corrosion" NACE-6 (ed. R A Rapp) 300-306; 1983, Houston, National Association of Corrosion Engineers.

10 Barry T I, Chart T G, Research and Development of High Temperature Materials for Industry, 1989, E Bullock ed, Elsevier Applied Science, Amsterdam, The Netherlands, 565-592.

11 Rahmel A, Schoor M, Velasco-Tellez A, Pelton A, Oxidation of Metals, 1987, 27, 199-205.

12 Barry T I, Dinsdale A T, Mater. Sci. Technol.; 1994, 10, 1090-1095

13 Lobb R C, Evans H E, in "Plant Corrosion", (eds. J C Strutt & J R Nicholls), Ellis Horwood, Chichester, 1987, 275-288.

14 Atkinson A, Taylor R I, J. Phys. Chem. Solids, 1986, 47, 315-323.

15 Barry T I, Dinsdale A T, Gisby J A, JOM, 1993, 45, 32-38.

16 Barry T I, Bayliss R K, Lay L A, J. Matls. Sci., 1968, 3, 229-238

17 Cox M G C, McEneney B, Scott V D, Nature (Physical sciences), 1972, 337, 140-142.